Case study of failure of long prestressed precast concrete girder during lifting[1]

A. de la Fuente[1], J.M. Bairán[2], S.H.P. Cavalaro[3]

[1]Universitat Politècnica de Catalunya (UPC), Department of Civil and Environmental Engineering, Jordi Girona 1-3, C1, 08034. e-mail: albert.de.la.fuente@upc.edu
[2]Universitat Politècnica de Catalunya (UPC), Department of Civil and Environmental Engineering, Jordi Girona 1-3, C1, 08034. e-mail: jesus.miguel.bairan@upc.edu
[3]Loughborough University, Loughborough, United Kingdom, School of Architecture, Building and Civil Engineering, Sir Frank Gibb Building RT102. e-mail: S.Cavalaro@lboro.ac.uk

ABSTRACT

Improvements in concrete technology, reinforcing systems and manufacturing enable the use of longer reinforced precast concrete girders, contributing to the competitiveness of this solution for bridge decks. The weight of the girders should be limited in order to achieve an optimum between span length, transportation costs and lifting costs. The current tendency in design is to minimize the width of the flanges of the girder. This makes the element more flexible to lateral deformation and increases the risk of lateral instability in temporary situations without lateral supports. This is reflected in an increment of the number of accidents and damages associated with such phenomenon. The main objective of this study is to describe a real case study of lateral instability of a 46 m long prestressed concrete girder during lifting operations as well as to perform a parametric study to understand the limits of the problem observed. In addition to presenting the case study, simplified formulations and numerical simulations are used to assess the safety margins against lateral instability. Special attention is paid to the evaluation of the provisions gathered in codes and guidelines regarding the lateral stability since they might not cover extreme cases.

Keywords: concrete girders; lateral stability; lifting; failure; transient stages

1. INTRODUCTION

Precast, prestressed concrete girders (PPCGs) are commonly used in projects with demanding conditions in terms of construction speed and erection complexity. Several technological advances (e.g., materials, more efficient cross section shapes and larger prestressing strands) enable reaching larger spans with PPCGs (Castrodale and White, 2004). Because of the increase in span, the total weight of the PPCGs also increases, sometimes making the transport and handling stages the critical load cases in the structural design. The common strategy to overcome this issue is to minimize the weight of the PPCGs by reducing the width of the flanges. Nevertheless, this also reduces the minor-axis and torsional stiffness of the element, amplifying the risk of lateral instability.

The reported accidents and damages due to lateral instability are usually associated with eccentricities that activate second order effects during transient loading situations (lifting, transport, and support on bearings). Typical sources of eccentricities in PPCGs include (Bairán and Cladera, 2010): fabrication tolerances; variations in the lateral positioning of strands; local cracking; creep and shrinkage sweep; and sun heating on one side, causing the girder to bow. Since PPCGs were assumed to have enough margin of minor-axis stiffness, limited attention has been traditionally payed to the phenomenon.

---

1 Preprint. Please, cite this manuscript as:
de la Fuente A, Bairán JM, Cavalaro SHP (2019), "Case study of failure of long prestressed precast concrete girder during lifting", *Engineering Failure Analysis*, DOI:
https://doi.org/10.1016/j.engfailanal.2019.02.061

During the 1950's, several authors (Magnel, 1950; Billig, 1953; Leondhardt, 1955) came to the conclusion that a prestressed concrete beams with strands bonded to concrete could not buckle due to the prestressing force (Hurff, 2010), as there is no second order effect of this load and the cross-section of the element. Studies about lateral stability of PPCGs began in the 1950's. Initially, the sources of eccentricity were not taken into account in the formulations developed for the structural verification, assuming a failure due to lateral buckling of perfectly straight girders. In this context, Muller (1962) proposed an equation to compute the critical lateral buckling load for PPCGs. Anderson (1972) defined a factor of safety against lateral buckling which was slightly modified by Swann (1972) and Laszlo and Imper (1987). The analytical research carried out by Mast (1989 and 1993) was the first to consider the effect of initial eccentricity and to propose a safety factor accounting for the stiffness reduction due to cracking. This formulation is still in use today (e.g., PCI 2016).

With the advances on the computing systems and numerical methods, other approaches were proposed. Stratford and Burgoyne (1999a and 1999b) conducted an extensive numerical analysis for different support conditions (hanging beam, supported by bearings during transport and construction). They concluded that the hanging beam was the most critical support condition due to the absence of rotational restraint of the supports. They also proposed an analytical procedure to compute the tilt angle of a beam lifted by two cables, the associated lateral deflection and the additional stress generated (Stratford and Burgoyne, 2000). Later, the same authors studied the lateral stability of PPCGs supported by flexible bearings (Burgoyne and Stratford, 2001). Similarly, Plaut and Moen presented a set of analytical formulas for beams lifted by cables (Plaut et al., 2012; Plaut and Moen 2013) as well as unbraced beams on bearing pads (Plaut and Moen 2014). These formulations are valid for curved concrete and steel beams since, unlike previous studies, the torsional effects is also taken into account. Lee (2012) performed an extensive numerical analysis in which the thermal effects and the initial eccentricity were coupled. Finally, Chamorro and Aristiazabal 2016 proposed an analytical procedure to compute deflections and stresses for curved girders placed on non-linear elastic supports. Notice that none of these models included the nonlinearity of the concrete; hence, cracking is not explicitly considered.

In the field of the experimental research, Mast (1994) was probably also the first to develop a full-scale lateral bending tests on long-PPCGs. In this regard, an experimental program was conducted with a 45.4 m I-beam that was tested to failure to obtain the allowable tilt angle and calibrate the relationship between the tilt angle and the lateral cracked stiffness in order to assess a global safety factor. More recently, Hurff (2010) tested six rectangular PPCGs designed to fail by lateral-torsional buckling. The results showed that the prestressing strands did not restrain the beams from out-of-plane instability. After flexural cracking appeared, the beams buckled at a load significantly smaller than the predicted with elastic lateral-torsional buckling theory. Thus, initial imperfections proved to decrease the lateral-torsional buckling load. Another experimental program by Hurff and Kahn (2012) focused on the rollover stability of PCI BT-54 beams supported by elastomeric bearing pads. Rollover failure occurred well before an inelastic lateral-torsional buckling mode was anticipated, without showing evident signs of concrete cracking. Based on these results, the authors concluded that rollover is more critical than lateral-torsional buckling in case the ends of the PPCGs are not braced laterally. Another experimental program involving reinforced concrete beams was developed by Kalkan (2014) to calibrate an analytical solution that allows estimating the lateral torsional buckling load.

Design codes and guidelines have included specific provisions to prevent lateral instability of beams (eg. ACI 318-08, EN 15050:2008, *fib* Model Code 2010, Eurocode 2, PCI 2000, Spanish Code EHE-08, among others). Normally, these provisions appear in the form of geometrical relations that, if fulfilled, should guarantee the safety against lateral instability. Despite that, an increase in the number and the seriousness of damages or accidents with slender PPCGs in recent years has raised concerns about this phenomenon, underlying questions about the adequacy of such provisions. The study of the phenomenon and the assessment of reasonable magnitudes of girder span and support imperfections (PCI 2000) has become paramount to ensure safety during transient loading situations (Hurff, 2010).

In this context, the objective of this study is to present a real case of failure of long-PPCG during lifting operations and to verify numerically if the analytical approach proposed by Mast (1993) is consistent with the behavior observed in reality. Moreover, the study aims to evaluate through a parametric numerical study if the provisions gathered in codes and guidelines to account for second order effects might be insufficient. First, an overview of the analytical approach proposed by Mast (1993) is presented. After describing the case study, this simplified formulation and more advanced numerical simulations are used to assess the safety margins against lateral instability. Results obtained with both approaches are compared with each other and with the provisions from codes and guidelines. Findings and conclusions derived from this work not only are evidence of a case of PPCG with lateral instability but also might serve as a reference to promote the improvement of current design codes and guidelines.

2. ANALYSIS OF LIFTING OF PRESTRESSED GIRDERS

Lateral instability is characterized by the lateral deformation of the cross-section at the middle of the span, creating sideways deflection. This phenomenon is particularly relevant in steel I-beams, which have low torsional stiffness. Conversely, concrete I-beams tend to have thicker webs and wider flanges, which lead to cross sections 100 to 1000 times stiffer in torsion than those of steel girders of the same shape (Mast, 1989). Therefore, torsional rigidity can be assumed in concrete girders. This allows converting a complex coupled torsional–bending buckling problem into a lateral bending equilibrium problem for the case of beams hanging from cables.

Lateral imperfections in the form of an initial eccentricity ($\boldsymbol{e_i}$) tend to cause the center of gravity of the beam (**G**) to be slightly shifted to one side of the roll axis, as depicted in Figure 1. When the hanging cables hold the girder in a point within the cross-section's plane, there is no torsional stiffness to balance the rolling moment generated. Consequently, the girder rolls about the element's axis in a solid movement, so the centroid tends to align with the hanging point to achieve equilibrium, forming an initial tilt angle $\boldsymbol{\theta_i}$ with the vertical axis. Part of the beam weight (**W**) is then applied at the minor-axis (**W**sin$\boldsymbol{\theta}$) and activates a lateral deflection, which further shifts **G** and increase the tilt angle due to second order effects. If the lateral bending stiffness is compatible with the magnitude of $\boldsymbol{e_i}$, the girder may reach equilibrium at a tilt angle $\boldsymbol{\theta_{eq}}$, slightly larger than angle $\boldsymbol{\theta_i}$. On the contrary, if the lateral bending stiffness is not enough, lateral deflection and lateral bending moment increase. This may produce cracking or even collapse.

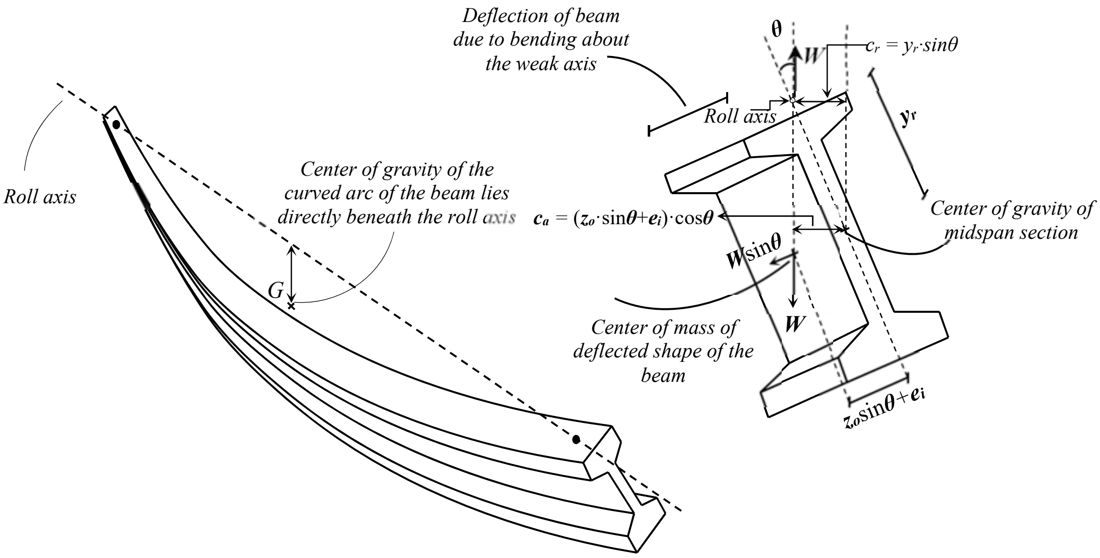

Figure 1. Final equilibrium position of a hanging girder [adapted from Mast, 1989]

The equilibrium tilt angle (θ_{eq}) can be assessed by means of successive approximations using equation 1, where y_r is the height of the roll-axis above **G**, and z_o is the lateral deflection of **G** of the curved beam caused by the full weight of the beam (**W**) applied to the weak axis. This consists in a second order analysis that can be easily programmed in any of the commercial packages available in the market, the input data being all those geometric and mechanical variables that define both the girder (and its cross-section) and also the constituent materials (concrete and active steel).

$$tan\theta_{eq} = \frac{(z_o sin\theta_{eq} + e_i)}{y_r} \quad (1)$$

In prestressed elements, the camber produces a negative effect because the centroid is closer to the rotating point, (Peart et al., 1992). Such effect can be considered by shifting **G** upwards a magnitude $\delta_G = 2\delta_P/3$ (δ_P is the total camber at the midspan expected when lifting operations are performed). Moreover, z_o can be calculated with equation 2, considering the positive effect of overhanging by moving the lifting points inwards a distance (a). In this equation, **E** is the Young Modulus of the concrete; I_{yy} is the weak-axis inertia; **L** is the total length of the girder; and $L_1 = L - a$.

$$z_o = \frac{W}{12EI_{yy}L}\left(\frac{1}{10}L_1^5 - a^2L_1^3 + 3a^2L_1 + \frac{6}{5}a^5\right) \quad (2)$$

Figure 1 represents the resisting moment arm (c_r) and the applied moment arm (c_a), which appears as a result of the lateral movement of the centre of mass of the deflected beam. Considering these two variables, a global factor of safety (**FS**) may be calculated according with equation 3. The safety factor against cracking (FS_{cr}) may be derived from equation 3 considering θ equal to the tilt angle at which the cracking is expected to occur (θ_{cr}). θ_{cr} should be assessed by rotating the midspan section until the flexural tensile strength of concrete (f_{ctm}) is reached at any point of the section. The factor of safety against failure (FS_u) may be calculated by tilting the beam beyond θ_{cr} till reaching a maximum tilt (θ_{max}) for which any of the constituent materials of the cross-section fails.

$$FS = \frac{c_r}{c_a} = \frac{(z_o sin\theta + e_i)cos\theta}{y_r sin\theta} \quad (3)$$

The effective lateral stiffness ($I_{yy,eff}$) considering the influence of cracking should be used in this calculations. One of the main conclusions derived from the numerical and experimental research conducted by Mast (1993) and Mast (1994) is equation 4 that should assess $I_{yy,eff}$ with acceptable accuracy.

$$I_{yy,eff} = \frac{I_{yy}}{1 + 2.5\theta} \quad (4)$$

$I_{yy,eff}$ and θ_u were obtained by using a numerical model that allows simulating the effects of the biaxial bending of a prestressed concrete cross-section with the real geometry and configuration of the reinforcement (de la Fuente *et al.*, 2012). However, the approximation $\theta_u = \sqrt{e_i/(2.5z_o)}$ proposed by Mast 1993 can be used to estimate FS_u without the need of any advanced numerical model. The maximum FS_u is reached for a $\theta_u = 9.20°$. However, the analytical results of more advanced numerical simulations demonstrate that values of θ_u close to 23.00° may occur. Experimental results (Mast, 1994) confirm that θ_u up to 32.00° may be found prior to failure.

3. CASE STUDY

This case study involved a 45.6 m-long PPCG with an I-shape constant cross-section with a height of 2.0 m and upper flange width of 1.20 m, as depicted in Figure 2. A cross-sectional area (A_c) of 0.58 m^2, a major inertia (I_{xx}) of 0.325 m^4 and a minor inertia (I_{yy}) of 0.021 m^4 around the centroid were calculated. The element was part of a road bridge with three different spans (20.45, 44.90 and 45.57 m) and an overall cross-section after construction composed by 4 girders and an upper reinforced concrete slab with 0.25 m of thickness.

The expected prestress force (**P**$_k$) at the moment of the lifting operations was approximately 8,514 kN (assuming 15% of losses). The equivalent vertical eccentricity of the strands with respect to the centroid of the cross-section (e_p) was 0.73 m according to the production drawings. The concrete mix was designed to reach a compressive strength (f_{ck}) of 60 N/mm^2 at 28 days. The estimated elastic modulus (**E**$_c$) of the concrete was 34,694 N/mm^2 and the average flexural tensile strength ($f_{ctm,fl}$) was 4.528 N/mm^2.

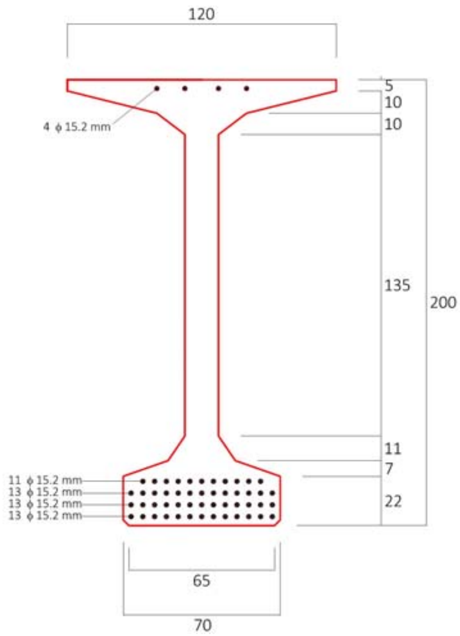

Figure 2. Dimensions (cm) and active reinforcement of the cross section.

Prior to the lifting operations, a visual inspection was conducted. An additional eccentricity (e_h) of approximately 12 mm of the lifting loops from the roll axis was identified. The total initial eccentricity (e_i) measured initially was 90 mm (equivalent to **L**/510). Since this complied with the EN 15050, the jobsite supervisor allowed the placement operations. The girder was lifted using two double-hoop cables placed at 2.0 m (a) from the ends with a height of 0.30 m (h_h). Two cranes were simultaneously used to guarantee a vertical alignment of the cables (ψ = 0°) and, therefore, avoiding the inclusion of an additional compressive force that would increase the likelihood of a lateral instability phenomena. In this process, a tilt was observed (Figure 3a) with a drastic increase of the lateral displacement up to 300 mm (**L**/150). The girder was placed again on the ground to evaluate possible damages (Figure 3b).

Figure 3. First lifting operation (a), deformed shape after first lifting (b) and deformed shape once in place after second lifting (c).

After another inspection, vertical cracks were observed at the left upper flange (where maximum tensile stresses are expected due to this phenomenon). Crack widths were over 0.40 mm, which should have been repaired in order to comply with the durability requirements if the element was finally accepted. A second intent of lifting was performed. This time, the girder was placed over the bearing pads of the pillars of the bridge (Figure 3c). However, it showed a lateral sweep of more than **L**/400, being unable to recover the original shape. This was probably caused by plastic deformation occurred during the lifting operations. Thus, the PCCG was rejected and a new girder was produced and transported to the jobsite. The new girder showed an initial total eccentricity of approximately **L**/590 and did not present any problem during the lifting operation.

4. PARAMETRIC STUDY

A parametric study considering a range of values of the lateral imperfection was conducted using the formulation by Mast (1993), as described in section 2. The total initial eccentricity assumed for calculation ranged between **L**/250 (182 mm) and **L**/1000 (45.6 mm). The total eccentricity of the centre of the gravity of the beam with the roll axis ($\boldsymbol{e_i}$) was assumed equal to the sum of the lateral sweep and the lateral eccentricity of the lifting hoops (12 mm). The results in terms of equilibrium tilt angle of the midspan section ($\boldsymbol{\theta_{eq}}$), the cracking tilt angle ($\boldsymbol{\theta_{cr}}$), the ratio $\boldsymbol{\sigma_{ct,max}/f_{ctm}}$ ($\boldsymbol{\sigma_{ct,max}}$ being the maximum tensile stress) and the cracking safety factor ($\mathbf{FS_{cr}}$) were then assessed. Figure 4 shows the curve relating $\boldsymbol{\theta_{eq}}$ and the ratio $\mathbf{L}/\boldsymbol{e_i}$, as well as $\boldsymbol{\theta_{cr}}$. A strong dependency between $\boldsymbol{\theta_{eq}}$ and $\mathbf{L}/\boldsymbol{e_i}$ is observed.

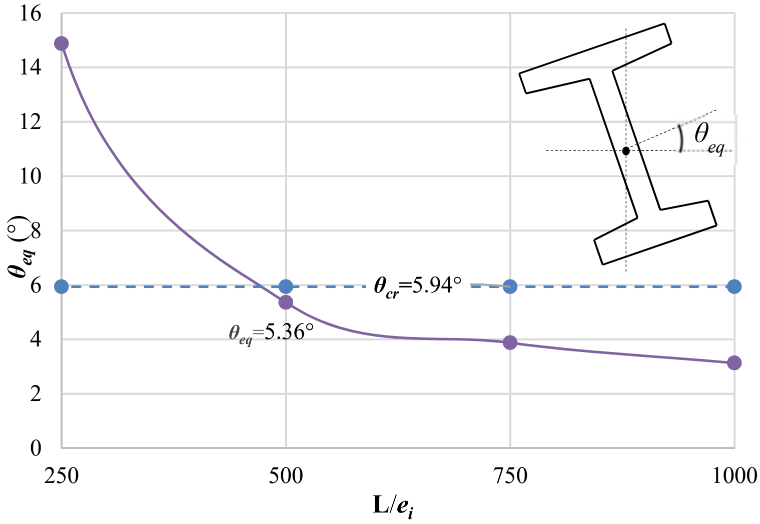

Figure 4. Relationship between θ_{eq} – L/e_i.

Values of θ_{eq} from 3.13° (**L**/1000) to 14.87° (**L**/250) may be found depending on **L**/e_i. Notice that θ_{eq} increases exponentially for e_i bigger than **L**/500. Likewise, θ_{cr} is only 10% bigger than that expected for **L**/500 (θ_{eq} = 5.36°). In fact, for a lateral imperfection **L**/475 the beam is expected to crack. This value may be easily reached prior to the lifting operations due to other phenomena that increase the total initial eccentricity, such as differential temperature (solar radiation) coupled with deformations induced by creep and/or shrinkage. In fact, a temperature gradient of 4.4ºC would be enough to produce this 10% increment.

Figure 5 shows the curve that relates the ratio $\sigma_{ct,max}/f_{ctm,fl}$ (left-hand y-axis) and $\mathbf{FS_{cr}}$ (right-hand y-axis) with **L**/e_i. As observed before, $\sigma_{ct,max}/f_{ctm,fl}$ increases exponentially for values of e_i bigger than **L**/500. In fact, for **L**/500, $\sigma_{ct,max}$ is just 20% above the expected $f_{ctm,fl}$ and $\mathbf{FS_{cr}}$ is 1.07. Although it satisfies the recommendations found in PCI 2016 ($\mathbf{FS_{cr}} \geq 1.00$), a high risk of cracking of the upper flange exists since an exponential increase of the ratio $\sigma_{ct,max}/f_{ctm,fl}$ is observed for **L**/e_i smaller than 500. The results confirm that the lifting configuration makes the beam prone to cracking and to lateral instability.

The fulfilment of the factor of safety should not be considered enough to prevent lateral instability of the PPCG analysed here. In fact, the element might comply with the factor of safety, remaining dangerously close to the point of exponential increase of stresses. In this case, small increases in the initial eccentricity induced by unaccounted factors (e.g., wind gust) during the lifting operations could lead to cracking or even the collapse of the element.

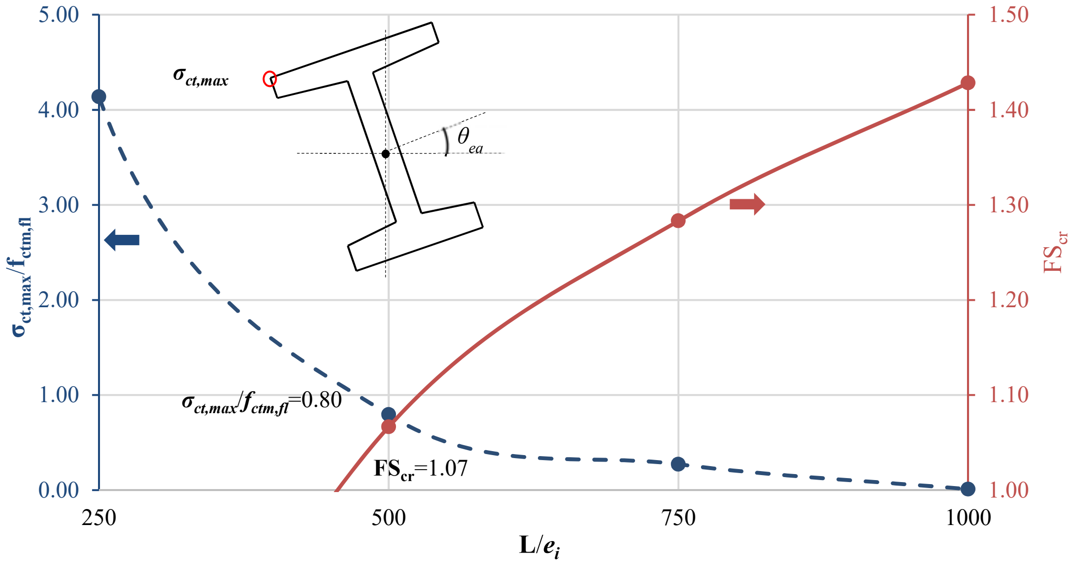

Figure 5. Relationship between $\sigma_{ct,max}/f_{ctm,fl} - L/e_i$ and $FS_{cr} - L/e_i$.

The girder described here did not collapse during the lifting operation due to safety margin between the cracking and the failure situations. To illustrate this, Figure 6 shows how the applied lever arm (c_a) and cracking resisting lever arm (c_r) vary with the tilt angle. The same figure also presents the factor of safety calculated as the ratio between c_r and c_a for different tilt angles, according with equation 3. Notice that the effective inertia also varies with the tilt angle according with equation 2.

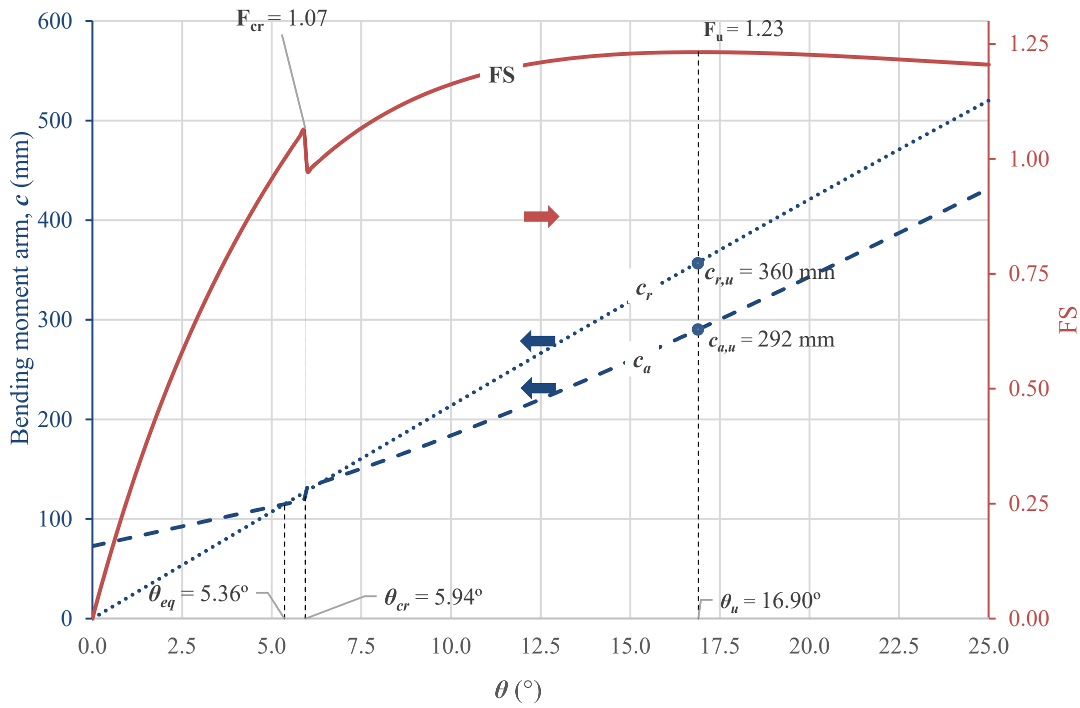

Figure 6. Relationship between $c - \theta_{eq}$ and $\mathbf{FS} - \theta_{eq}$.

As mentioned previously, the factor of safety against cracking is 1.07. Cracking would be reached for a tilt angle of 5.94°, which is slightly above the equilibrium tilt angle of 5.36°. The safety factor against failure (**FS$_u$**) is the maximum value found in Figure 6, which is 1.23 for a tilt angle θ_u of 16.90°. This means that a tilt angle of at least 16.90° should be reached in order for failure to take place.

This safety margin calculated according with the simplified formulation proposed by Mast (1993) was compared with that obtained from a nonlinear analysis considering the contribution of concrete and steel. A parabolic stress-strain diagram in compression and a brittle cracking in tension were assumed for the concrete. An elasto-plastic stress-strain diagram in compression and in tension were considered for the steel reinforcement. Several numerical simulations using the AES (Analysis of Evolutive Sections) model described in de la Fuente *et al*. (2012) were performed to obtain the interaction bending moment diagram shown in Figure 7. In the same figure, a dotted line indicates the path experienced by the girder as the tilt angle increases.

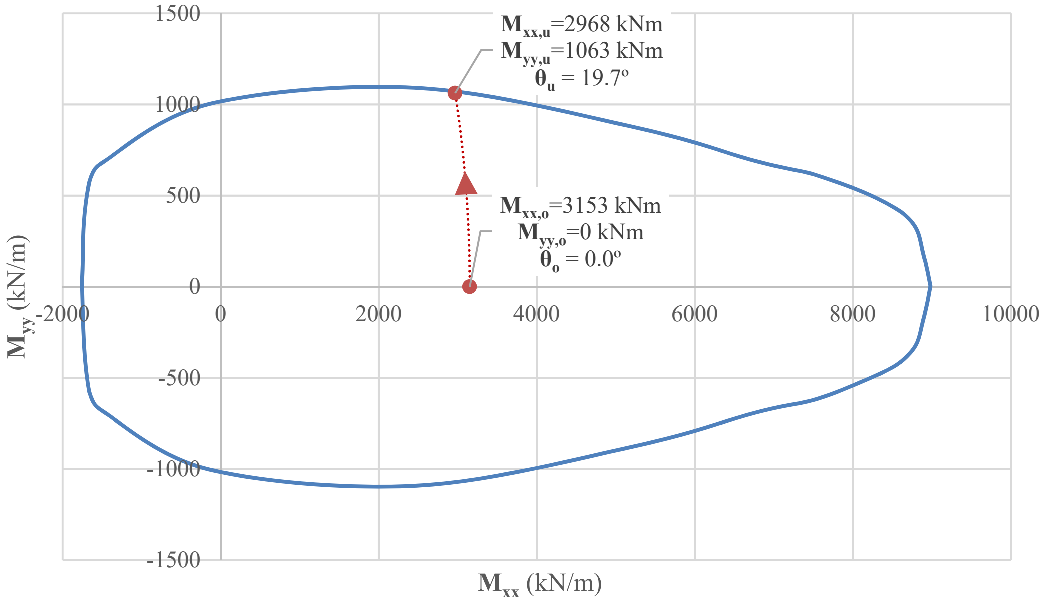

Figure 7. Interaction diagram (N = 0) and $\mathbf{M_{xx}} - \mathbf{M_{yy}}$ trajectory.

The results show that failure is expected for a tilt angle of 19.7°. The latter is 14% bigger than the 16.9° found with the formulation by Mast (1993) valid for vertically symmetric sections. This confirms that, despite the simplifications assumed for its deduction, the formulation by Mast (1993) provides a fair approximation of extreme cases of lateral deformability of a girder.

This sensitivity analysis has been performed respect to the total lateral eccentricity respect with the roll axis (e_i); nonetheless, it must be highlighted that variations of other geometric variables can also govern the stability phenomena:

- Position (a = 2.0 m), height (h_h = 0.30 m) and eccentricity (e_h = 12 mm) of the lifting hoops
- Angle of the lifting cables (ψ = 0.0º).
- Lateral eccentricity of the equivalent prestress tendon, assumed null in this study case.

Likewise, it is emphasized that other additional stability checks, similar to that performed in this analysis, must be performed in the design stage for transport, placing and other transient situations in which the girder is prone to suffer from lateral stability problems.

5. COMPARISON WITH PROVISIONS FROM CODES AND GUIDELINES

The provisions established in some codes and guidelines to prevent lateral instability of girders are summarized in Table 1. The table also shows the values measured in the case study or estimated through the numerical analysis. Even though the Annex 11 of the Spanish Code EHE-08 is not mandatory, it is the only one whose recommendation is not fulfilled for the PPCG described in the case study and indicate a potential problem due to lateral instability. The provisions of all other codes and guidelines contemplated in this work are fulfilled, suggesting that lateral instability is not expected. Such outcome contradicts the findings of the visual inspection and the results of the numerical analysis, thus leading to potentially unsafe prediction of the behaviour of the PPCG.

Table 1. Provisions from codes and guidelines to prevent lateral instability and values for case study.

Code or guideline	Recommendation	Value for real case study	Conclusion
EN 15050:2008	$e_i \leq \frac{L}{500}$	$e_i = \frac{L}{510}$	Fulfilled
Eurocode 2*	$\frac{L}{b} \leq \frac{70}{(h/b)^{\frac{1}{3}}}$	$38 \leq 59$	Fulfilled
	$\frac{h}{b} \leq 3.5$	$1.7 \leq 3.5$	Fulfilled
fib Model Code 2010*	$\frac{L}{b} \leq \frac{50}{(h/b)^{\frac{1}{3}}}$	$38 \leq 42$	Fulfilled
ACI 318-08*	$\frac{L}{b} \leq 50$	$38 \leq 50$	Fulfilled
PCI 2016	$FS_{cr} \geq 1.00$ $FS_u \geq 1.50$	$1.07 \geq 1.00$ $1.23 < 1.50$	Fulfilled Not fulfilled
Spanish Code EHE-08 (Annex 11)	$e_i \leq \frac{L}{750}$	$e_i = \frac{L}{510}$	Not fulfilled

* ***b*** and ***h*** being the width of the upper flange and h the height of the cross section, respectively

6. CONCLUSIONS

This study presents a real case study of a long PPCG with lateral instability problems. The numerical simulations and the structural verifications performed confirm the causes of the damages observed during the lifting operations. The following conclusions may be derived based on the results from this study.

- The current tendency of stretching PPCGs whilst maintaining the same cross-sections available in traditional catalogues increases the risk of lateral instability. The analysis conducted with the assumptions proposed in this paper confirms the small safety margin of the element during the lifting exists. Therefore, additional measures should be taken in order to prevent such problem.

- Despite complying with the requirements of several codes and guidelines, the girder analysed here showed cracking and non-recoverable deflections as a result of lateral instability during lifting. These results suggest that the allowable lateral imperfections and the criteria to disregard the influence of second order effects defined in codes and guidelines should be revised in accordance with new trends.

- The stresses applied in the cross section increases exponentially with the initial eccentricity. Like in the case study, an element might comply with the factor of safety against cracking but could be dangerously close to the point of exponential increase of stresses. In this situation, small increments in the initial eccentricity, not accounted for in the design, may lead to cracking or even collapse. Therefore, the fulfilment of a certain factor of safety should not be considered enough to prevent lateral instability. Additional structural verifications should be performed for different initial eccentricities to evaluate how close the PPCG is of cracking for small increments of the eccentricity.

- The numerical simulation performed with the program AES confirm that the formulation proposed by Mast (1993) provides a fair approximation of extreme cases of lateral deformability of a girder, as the one observed here. Such formulation may be used for simplified evaluations of the risk of lateral instability.

REFERENCES

ACI Committee 318, "Building Code Requirements for Structural Concrete (ACI 318-02) and Commentary (318R-02)," American Institute, Farmington Hills, Michigan, 2002, 443 pp.

Anderson, A. R. "Lateral stability of long prestressed concrete beams". PCI Journal, 16(3), 7-9. May-June 1971.

Bairán, J. M. and Cladera, A. (2014). "Collapse of a precast concrete beam for a light roof. Importance of elastomeric bearing pads in the element's stability." *Eng. Failure Analysis*, 39, 188-199.

Billing, K. (1953). *Prestressed Concrete*. D Van Nostrand Company, Inc., New York.

Burgoyne, C. J., Stratford, T.J. (2001). "Lateral instability of long-span prestressed concrete beams on flexible bearings". The Structural Engineer, Volume 79/No 6, March 2001.

Castrodale, R. W. and White, C. D. "Extending Span Ranges of Precast Prestressed Concrete Girders". National Cooperative Highway Research Program, Report 517. Washington D. C., 2004.

Chamorro, E., Aristiazabal, J.D. (2016). "Analysis of a horizontally curved long-span beam on two nonlinear elastic supports." J. Bridge Eng. 21(5): 1-14.

de la Fuente, A., Aguado, A., Molins, C., and Armengou, J. (2012). "Numerical model for the analysis up to failure of precast concrete sections." *Comput. Struct.*,106-107, 105-14.

EHE-08. Comisión Permanente del Hormigón. *Instrucción de Hormigón Estructural*. Ministerio de Fomento. 3th Edition, 2009.

EN 15050:2008 +A1:2012. *Precast concrete products – Bridge elements*.

fib Bulletins 65-66, *Model Code 2010*. Final Draft, 2010. fédération internationale du béton (fib), Lausanne, Switzerland.

European Committee of Standarization. *Design of concrete structures – Part 1-1: General rules and rules for buildings*. Eurocode 2, Brussels, 2004.

Hurff, J. "Stability of Precast Prestressed Concrete Bridge Girders Considering Imperfections and Thermal Effects". Georgia Institute of Technology, School of Civil and Environmental Engineering, August 2010.

Kalkan, I. (2014). "Lateral torsional buckling of rectangular reinforced concrete beams." ACI Struct. J. 111, pp.: 71-82.

Lee, J.H. (2012). "Behaviour of precast prestressed concrete bridge girders involving thermal effects and initial imperfections during construction." *Eng. Struct*. 42: 1-8.

Laszlo, G. and Imper, R. R. "Handling and Shipping of Long Span Bridge Beams". PCI Journal, November-December 1987, pp. 86-101.

Leonhardt, F. (1955). *Spannbeton für die Praxis*. Verlag Von Wilhelm Ernst&Sohn, London.

Magnel, G. (1950). *Prestressed Concrete*. Concrete Publications Limited, London.

Mast, R. F. (1989). "Lateral Stability of Long Prestressed Concrete Beams, Part 1." *PCI J*. 34(1), 34–53.

Mast, R. F. (1993). "Lateral Stability of Long Prestressed Concrete Beams, Part 2." *PCI J*., 38(1), 70–88.

Mast, R. F. (1994). "Lateral bending test to destruction of a 149 ft. prestressed concrete I-beam." *PCI J*., 39(1), 54-62.

Muller, J. "Lateral Stability of Precast Members During Handling and Placing". PCI Journal, February 1962, pp. 20-31.

Peart, W.L., Rhomberg, E.J., James, R.W. (1992). Blucking of suspended camber girders. *ASCE J Struct. Eng.* 118(2): 505-528.

PCI. *Tolerance Manual for Precast and Prestressed Concrete Construction*. Precast Concrete Institute, Chicago, IL. 1st ed., 2000.

PCI. *Recommended practice for lateral stability of precast, prestressed concrete bridge girders* (CB-02-16). PCI committee on Bridges. 2016.

Plaut, R. H., Moen, C. D., Cojocaru, R. (2012). “Beam deflections and stresses during lifting." *Eng. J.*., 49(4), 187-194.

Plaut, R. H., Moen, C. D. (2013). “Analysis of elastic, doubly symmetric, horizontally curved beams during lifting." *J. Struct. Eng*., 139(1), 39-46.

Plaut, R. H., Moen, C. D. (2014). “Stability of unbraced concrete beams on bearing pads including wind loading." *Eng. Struct*., 69, 246-254.

Stratford, T.J., Burgoyne, C. J. (1999a). "Lateral stability of long precast concrete beams". *Proc. Instn Civ. Engrs Structures & Bldgs*, May-August 1999, 124, pp. 169-180.

Stratford, T.J., Burgoyne, C. J. (1999b). "Stability design of long precast concrete beams". *Proc. Instn Civ. Engrs Structures & Bldgs*, May-August 1999, 134, pp. 159-168.

Stratford, T. J., and Burgoyne, C. J. (2000). “The toppling of hanging beams.” *Int. J. Solids Struct*., 27(26), 3569-3589.

Swann, R. A., Readers comment to "Lateral Stability of Long Prestressed Concrete Beams", PCI Journal, 16(6), November-December 1971.